

GENERAL FEATURES OF NEUTRINO EXPLOSION DYNAMICS

REVEALED BY SUPERNOVA 1987A

S. A. Bludman and P. J. Schinder

Department of Physics, University of Pennsylvania
Philadelphia, Pa. 19104
USA

ABSTRACT

The general features of neutrino transport models for Type II supernova are reviewed, distinguishing the conditions necessary for a prompt shock or for a delayed shock explosion mechanism. The arrival times and energies of Supernova 1987A are consistent with iron core collapse to a neutron star and with known properties of neutrinos. A massive star collapse in our Galaxy, whether or not accompanied by an optical display, would test particular theories for supernova dynamics and for weak interactions.

I. IRON CORE COLLAPSE AND SUPERNOVA EXPLOSION DYNAMICS

A. Late Stages of Stellar Evolution. All of the general features of the quasistatic evolution of a nondegenerate star of mass M and radius R are determined by the virial theorem relating the mean kinetic and potential energies:

$$\langle 2K \rangle = - \langle V \rangle \sim GM^2/R, \quad E = \frac{1}{2} \langle V \rangle \sim - GM^2/2R.$$

For a nondegenerate star of N baryons of mass m_H ,

$$\langle K/N \rangle = \frac{3}{2} \langle kT \rangle \sim \frac{GM m_H}{R} \sim M^{2/3} \langle \rho \rangle^{1/3}$$

where $\langle \rho \rangle$ is the mean density. Four immediate consequences are:

- (1) In order to contract gravitationally, any star must radiate energy. In late stages of stellar evolution (carbon burning and later), the neutrino radiation dominates that by photons.
- (2) In nondegenerate stars, this energy loss leads to temperature increase. (Nondegenerate stars show a negative heat capacity.) If collapse continues, this temperature increase ignites successively nuclear fuels
 $H \rightarrow He \rightarrow C \rightarrow O-Ne-Mg \rightarrow Si-S \rightarrow Fe$.
- (3) Because of the temperature gradient between the center and surface, a star evolves an onion-skin structure with a large envelope of unburnt hydrogen, surrounding a He shell, surrounding a O-Ne-Mg shell...all the way up to Fe, if the star is massive enough to continue contracting.
- (4) Because nuclear burning rates increase rapidly with temperature, nondegenerate stars are gravitationally stable: any density perturbation is immediately corrected by a change in nuclear burning rate and in pressure. A degenerate star has, however, lost this stability: as long as it remains degenerate, its pressure is not responsive to temperature; as soon as the temperature rises enough to remove the degeneracy, the thermal pressure turns on explosively. The ignition temperature of each successive nuclear fuel increases with z^2 . In low mass stars, a given fuel will ignite at low density, non-degenerately; this allows the star to evolve quiescently to the next stage of nuclear burning.

For $M < 8 M_\odot$, carbon ignition taking place while the electrons are degenerate, leads to nuclear explosion. For $8 M_\odot < M < 12 M_\odot$ (?), carbon burns non-degenerately, but O-Ne-Mg burning takes place explosively. For $12 M_\odot$ (?) $< M$, all fuels burn nondegenerately and the core can evolve quiescently all the way to Fe, the stablest of nuclei. Only these massive stars ($> 12 M_\odot$), ultimately producing type II supernovae by Fe core collapse, will be considered in this article. More particularly, we will concentrate on the collapse and explosion of this $1.2-2.0 M_\odot$ iron core, ignoring the

stellar mantle and envelope in which the supernova light is produced.

Evolutionary calculations⁽¹⁾ show that a star of main-sequence mass $M_{MS} = 13 M_{\odot}$ evolves a helium core of $M_{\alpha} = 3.3 M_{\odot}$ and an iron core of $M_{Fe} = 1.17 M_{\odot}$. At the center, the density is $\rho_c = 3 \times 10^{10} \text{ g cm}^{-3}$, the temperature is $T_c = 0.78 \text{ Mev}$, and the electron-baryon ratio is $Y_{ec} = 0.41$. During late stages of evolution, electron capture ($e^- + p \rightarrow e^- + n$) during quasistatic evolution has already neutronized iron from $Y_e = 0.46$ for Fe^{56}_{26} down to $Y_e = 0.41$ for a mixture of neutrino-rich Fe-Ni. Analysis of the light curve of Supernova 1987A shows that its progenitor was somewhat more massive: $M_{MS} = (15-20)M_{\odot}$, $M_{Fe} = (1.3-1.4)M_{\odot}$.

B. Core Collapse. Stripped of its surrounding onion-skins of lower mass elements, the iron core of the massive star would be a white dwarf. Although its mass exceeds the cold Chandrasekhar mass $M_{CH} = 5.75 Y_e^2 M_{\odot} = 1.01 M_{\odot}$, the iron core is supported against gravity by the thermal pressure of its nuclei and by semi-degenerate electrons. This heat content now reverses the exothermic reactions that produced the iron core in the first place by nuclear fusion. Initiated by endothermic thermal dissociation of the iron nuclei, followed by accelerated electron capture, the reduction in both thermal and degeneracy pressure support drives the core into runaway collapse. Even after neutrinos are trapped at $\rho_{TR} = 10^{12} \text{ g cm}^{-3}$, the cataclysmic collapse accelerates. The collapsing core separates into a subsonic inner core of mass $M_{HC} = 1.04 M_{Fe} (Y_L/Y_{ei})^2$, which collapses homologously, and a supersonic outer core of mass $M_{OVER} = M_{Fe} - M_{HC}$, which lags behind. Here Y_{ei} is the initial electron fraction and $Y_L = (Y_{ef}^{4/3} + 2^{1/3} Y_f^{4/3})^{4/3}$ is the effective lepton fraction of the trapped neutrinos and electrons.

Nuclear incompressibility halts the homologous collapse of the core when the central density reaches $\rho_b \sim (3-4)x$ (nuclear saturation density) $\sim 9 \times 10^{14} \text{ g cm}^{-3}$. The signal that the center has stopped propagates through the subsonic inner core, but cannot reach beyond the sonic point, outside of which the matter is falling faster than sound speed. Near this sonic point, which is just outside the edge of homology defined by the included mass M_{HC} , a pressure wave builds up that quickly steepens into a shock wave. The original source of this shock energy is the compressional energy, $E_{comp} \sim 7 \times 10^{51} \text{ ergs}$, of the compressed nuclear matter. The shock is nourished by the energetic matter falling through it and starts to propagate outwards.

The precise location of the sonic point or of the edge of the homology M_{HC} depends on the deleptonization that has transpired from initial electron fraction Y_{e1} to lepton fractions Y_{ef}, Y_{vf} at bounce. As the shock wave propagates through the mass overlay M_{OVER} , it is depleted by neutrino radiation $E_{\nu}^{rad} \approx (2-4) \times 10^{51}$ ergs and by nuclear dissociation $E_{diss} = 8.5 (M_{OVER}/0.5 M_{\odot}) \times 10^{51}$ ergs.

C. Shock Propagation. The subsequent fate of the shock propagating through the overlay depends sensitively on neutrino radiation hydrodynamics and is still problematical. If (1) the nuclear matter is compressible enough at high density ρ_b to make the original shock energy E_{comp} large; (2) the infall deleptonization is small, so that M_{HC} lies far out; (3) the initial core mass is small, so that $M_{OVER} = M_{Fe} = M_{HC}$ is tolerably small, then the shock will traverse to the edge of the compact iron core with sufficient energy to eject a superficial layer of iron with kinetic energy $\sim 3 \times 10^{51}$ ergs, sufficient to power the optical display of the supernova envelope. This direct, essentially hydrodynamic mechanism, is called the prompt mechanism because if it succeeds, it operates on hydrodynamics time scales of tens of milliseconds.

Otherwise, the shock stalls at about 200-300 km. Because the tenuous matter outside this large radius is weakly bound gravitationally, it may be ejected, if the stalled shock is revived by neutrinos diffusing out of the hot inner core below and by matter still infalling from above. This mechanism is called the delayed or revived mechanism and operates on the time scale (~ 1 second) for neutrinos to diffuse out of dense matter.

Whether either the prompt or the delayed mechanism succeeds well enough to eject matter and power an optically visible supernova is still theoretically undecided. We will return to this question of neutrino explosion dynamics in the second lecture.

D. Prospectus. The gravitational energy ultimately released when an extended structure collapses down to a compact neutron star, is the neutron star binding energy of $(3-5) \times 10^{53}$ ergs. At least 99% of this energy emerges as neutrinos. Even if an optical supernova of 10^{49} ergs is formed, this requires conversion of only 1% of the $(3-5) \times 10^{53}$ ergs into ejected kinetic energy, which subsequently converts into light with another 1% efficiency. The optical supernova, dramatic as it is, is only a superficial phenomenon very sensitive to the neutrino-matter coupling at the edge of the iron core and the matter-light coupling in the surrounding stellar

envelope. The huge neutrino signal is, on the other hand, relatively insensitive to details.

What characterizes stellar collapse is this huge neutrino output in a few seconds. Indeed, Supernova 1987A shows us how a supernova can be optically weak, so that the true collapse rate may be seriously underestimated by the observed supernova rate. It also reminds us that massive stars may collapse to neutron stars with little or no light emission and that some collapses into black holes may radiate neutrino pulses, before they are engulfed by the event horizon.

If a neutron star remains, it must be very hot (~100 Mev) and must cool rapidly by neutrino radiation. It is these neutrinos from the hot nascent neutron star that were observed by Kamiokande II and IMB. We turn now to the analysis of the arrival times and energies of the $11 + 8 = 19$ neutrinos they observed. We will find that the sparse and uncertain neutrino signals from the cooling neutron star suffice to confirm remarkably the general features of the scenario we have just described, but not the details of any particular theoretical neutrino explosion mechanism.

II. ANALYSIS OF THE NEUTRINOS FROM SN 1987A

A. Neutrino Arrival Times and Energies. In our^(2,3,4) analysis of the Kamiokande II and IMB data we: (1) considered indiscriminately the complete sample of 19 neutrinos; (2) Ignored their angular distribution, which is consistent with isotropy. (Almost all the events captured in water would be expected to be $\bar{\nu}_e$ absorption ($\bar{\nu}_e + p \rightarrow e^+ + n$); only about one event would be expected to be $\nu_e + e^- \rightarrow \nu_e + e^-$. This might be the first forward-pointing event of Kamiokande II but, because we have no way of discriminating, we treated all 19 events as coming from the same $\bar{\nu}_e$ sample); (3) We set the neutrino mass equal to zero. The signal direction is consistent with $m_{\nu_e} < 17$ eV, which is also the laboratory limit.

We avoided the theorists' temptation to overinterpret these 19 events and did not pretend to discriminate among the 19 neutrinos. We assumed a thermal distribution of $N_o \bar{\nu}_e$ with temperature T_s at time $t = 0$ at the source, and folded in the individual detector thresholds, efficiencies and energies and their uncertainties. We fit the thermal source cooling to the cooling function

$$T(t) = T_s (1 + \frac{at}{n})^{-n} \quad (2.1)$$

where, for each n , the three parameters T_s , a , N_o were determined from the data by maximum joint likelihood analysis. Special cases of the above form are: $a = 0$, constant temperature; $n = \infty$, exponential cooling at the

constant rate $\tau = a$; $n < \infty$, power law cooling, at the rate

$$\tau(t) \equiv -(\ln t / dt)^{-1} = a^{-1} + t/n,$$

fast at the beginning, but protracted thereafter; $n = 1/2$, semi-degenerate Fermi gas whose heat content $E(t) \propto T^2$ is being black-body radiated $dE/dt = 4\pi R_\nu^2 \sigma T^4$ from some neutrinosphere fixed at (average) radius R_ν .

Our best maximum likelihood fits to the combined Kamiokande-IMB data are given in Table 1 for each n , together with their (unnormalized) likelihoods. We see that:

- (1) The cooling models for various n have comparable likelihood. Any cooling source is 10^5 times more likely than a constant temperature source radiating for 12.4 seconds.
- (2) Our exponential fit yielding a fluence of $N_0 = 4.6 \times 10^{57} \bar{v}_e$ with energy $E = 6.7 \times 10^{52}$ ergs agrees with that of Spergel et al. (5)
- (3) Our $n = 1/2$ model (semidegenerate gas radiating from a black body of fixed radius), $T(t) = T_S (1 + 2at)^{-1/2}$, $T_S = 4.1$ Mev, $a = 0.12 \text{ s}^{-1}$ $N_0 = 7.8 \times 10^{57} \bar{v}_e$, $E_0 = 8.0 \times 10^{52}$ ergs is three times more likely than the exponential model, for which there is no theoretical basis.
- (4) Allowing for six neutrino flavors, the total energy radiated $6 E_0 = (4-5) \times 10^{53}$ ergs, in good agreement with the binding energies of neutron stars of maximum mass calculated with various equations of state.
- (5) Because of the power-law tail to its cooling curve, the $n = 1/2$ model

n	a (s^{-1})	T_S , (Mev)	E_0 (10^{52} erg)	N_0 ($10^{57} \bar{v}_e$)	Max(J)
0.335	0.176	4.20	11,9	380.6	6.304
0.35	0.167	4.19	10.9	41.4	6.376
0.4	0.144	4.16	9.2	13.1	6.380
0.5	0.116	4.08	8.0	7.8	5.940
1.0	0.077	3.95	7.1	5.3	4.075
2.0	0.063	3.88	6.9	4.9	3.066
∞	0.052	3.84	6.7	4.6	2.197
-	0	3.33	5.7	3.4	10^{-5}

Table 1. Maximum joint likelihood fit of our cooling models $T = T_S (k + \frac{at}{n})^{-n}$. Special cases: $a = 0$, constant temperature, $n = \infty$, exponential; $n = \frac{1}{2}$ semidegenerate Fermi gas radiating as a black body.

gives E_o and a neutron star binding energy 20% higher than that given by exponential cooling. This large binding energy suggests a large mass (1.4 M_\odot) iron core and a soft nuclear equation of state.

The probable errors in each of our best fits were 10% in T_s , 30% in E_o and in N_o , determined by running 750 Monte Carlo simulations of the two detectors.

The goodness-of-fit between our best fit $n = 1/2$ model and the separate Kamiokande II and IMB data sets is shown in Fig. 1. The top two curves show the cumulative distribution in arrival times, the bottom two curves the cumulative distribution in energies for the 11 Kamiokande II events and for the 8 IMB events. In each figure, the best fit is given by the central (dotted) curve, the 1σ and 2σ limits are shown by the surrounding pairs of long-dashed and short-dashed curves. Although Kamiokande seems to detect fewer and IMB more events than our best fits would have predicted, the observations at each detector agree with our best joint fit within 1σ . All our models would show almost the same goodness-of-fit.

B. Other Conclusions. Kamiokande II knew the absolute time of their data train only within one minute. We therefore estimated the time offset between the Kamiokande II and IMB data trains by Monte Carlo simulations and found that Kamiokande II lagged IMB by 0.1 ± 0.5 s. Our analysis of the data thus sets the Kamiokande clock within 0.5 seconds!

Besides the above continuous cooling models, we also considered models in which, as theoretically expected, a short heating period preceded the cooling. We found that such heating period in the observed data had to be shorter than 0.4 s.

By power spectrum analysis and by minimum residuals, we also showed that there were no significant periods in the Kamiokande II data, on any time scale.

The temperature of the $\bar{\nu}_e$ neutrinosphere is maintained by ν_e and $(-\bar{\nu}_e)$ diffusing out of the inner core over a few seconds. The total energy radiated, $6 E_o$, and the $\bar{\nu}_e$ number flux cooling time $(3a)^{-1} = (2.5-6)$ seconds we obtained, are consistent with neutrino diffusive cooling of a hot neutron star of time-averaged radius 35 ± 10 km.

The sparse and uncertain data from Kamiokande II and IMB are then consistent with the diffusive cooling of a hot neutron star remnant from the collapse of a $1.4 M_\odot$ iron core in a massive star. The observations are also consistent with laboratory bounds on the ν_e mass and with cosmological bounds on axion coupling, but no neutrino mass, neutrino oscillations, exotic neutrino interactions or exotic particles can be demonstrated from the

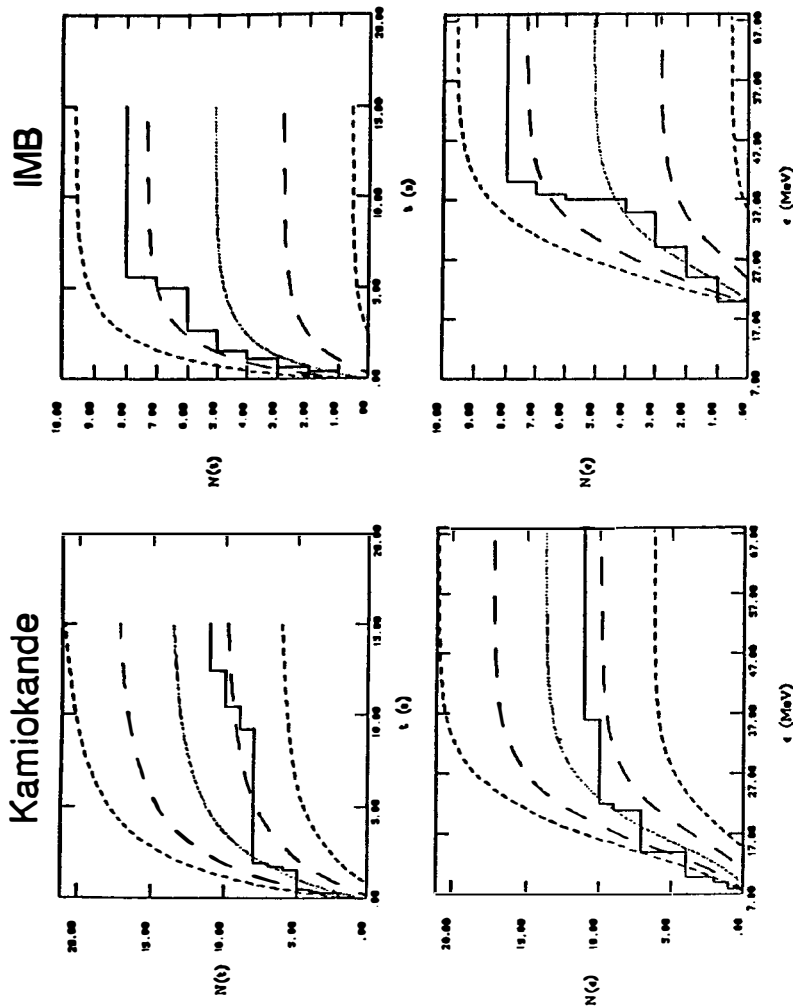


Fig. 1. Comparison of best fit $n = 1/2$ model with observations.

SN 1987A data. The data is also too sparse to show the detailed time structure that would test any particular neutrino explosion mechanism.

III. PROSPECTS FOR STELLAR COLLAPSES WITHIN OUR GALAXY.

Within our Galaxy, all stars more massive than $10 M_{\odot}$ die at a rate 1/50 years, a value as small as 1/11 years being estimated by Bahcall and Piran.⁽⁶⁾ These collapses may be to black holes as well as to remnant neutron stars or pulsars. Protracted mass accretion leading finally to black hole formation might be expected to produce a neutrino signal similar to SN 1987A, whether or not associated with optically visible supernova.

Any stellar collapse within our Galaxy, ten times closer than SN1987A in the Large Magellanic Cloud, would produce about 10^3 neutrinos in the existing Kamiokande-IMB detectors. With so many events, important particle physics and supernova physics would be learned.

A. Particle Physics. A sample of 10^3 supernova neutrinos would contain about 14 $\bar{\nu}_{\mu, \tau}$ whose masses could be determined from their time of flight

$$\Delta t = \left[\frac{m_{\nu}(\text{eV})}{E_{\nu}(\text{MeV})} \right]^2 \left(\frac{D}{5 \text{ kpc}} \right) 0.25 \text{ seconds}$$

from distance D. Indeed, if $\nu_{\mu, \tau}$ have masses below the cosmological bound, their masses could be directly measured only over astronomical flight paths.

B. Supernova Physics. A pulse of 10^3 neutrinos would show time structure (prompt neutronization burst over milliseconds, accretion heating and diffusive cooling over seconds) diagnostic for different theoretical neutrino explosion mechanisms. In some models⁷, the delayed explosion is preceded by gravitational oscillations of period 0.1 seconds, characteristic of the inner core density. If so, the same power spectrum analysis which revealed no periods in the 11 Kamiokande II events would reveal such 0.1 second periods provided their amplitude modulation $> 10\%$.

For these reasons, we look forward to the construction of dedicated supernova detectors and the coming Galactic supernova. Armed with the experience and confidence gained from Supernova 1987A, the new cadre of neutrino astrophysicists will be able to observe and analyze neutrino dynamics important to both supernova and particle physics.

This work is partially supported by the DOE contract EY-76-D-02-3071.

References

1. K. Nomoto, T. Shigeyama, and M. Hashimoto, in Proc. ESO Workshop on "SN 1987A" (ed. I. J. Danziger, ESQ: Garching (1987)).
2. S. A. Bludman and P. J. Schinder, Ap. J. 326, 265 (1988).
3. P. J. Schinder and S. A. Bludman, in Proc. Fourth George Mason Fall Workshop in Astrophysics (Cambridge Univ. Press, 1988).
4. S. A. Bludman and P. J. Schinder in Proc. Workshop on Extrasolar Neutrino Astronomy (UCLA, 1987).
5. D. N. Spergel, T. Piran, A. Loeb, J. Goodman and J. N. Bahcall, Science 237, 1471 (1987).
6. J. N. Bahcall and T. Piran, Ap. J. (Letters) 267, L77 (1983).
7. R. Mayle, Ph.D. Thesis, University of California, Berkeley, 1986.